Core–Shell Multiwalled Carbon Nanotube/Cobalt Corrole Hybrids for the Oxygen Reduction Reaction

Paul-Gabriel Julliard, Manel Hanana, Laurent Alvarez, Renaud Cornut, Bruno Jousselme, Gabriel Canard, Stéphane Campidelli

Core-shell multi-walled carbon nanotubes/cobalt corroles hybrids for oxygen reduction reaction

Paul-Gabriel Julliard,[‡] *Manel Hanana,*[#] *Laurent Alvarez,*[¶] *Renaud Cornut,*[#] *Bruno Jousselme,*[#] *Gabriel Canard,*[‡,*] *and Stéphane Campidelli*[#,*]

[‡]Aix Marseille Univ, CNRS, CINaM UMR 7325, AMUtech, Campus de Luminy, 13288 Marseille, France.

[#]Université Paris-Saclay, CEA, CNRS, NIMBE, LICSEN, 91191, Gif-sur-Yvette, France.

[¶]Laboratoire Charles Coulomb (L2C), CNRS-Université de Montpellier, 34095, Montpellier, France.

Corresponding authors: stephane.campidelli@cea.fr, gabriel.canard@univ-amu.fr

KEYWORDS. carbon nanotubes, cobalt corroles, oxygen reduction reaction.

ABSTRACT. The development of hybrid nanomaterials that preserve and combine the properties of their constituents is a central issue of nanosciences. Herein, we describe the polymerization *via* CuAAC (copper-catalyzed azide-alkyne cycloaddition) of cobalt(III) corroles around conductive carbon nanotubes to produce chemically robust hybrid catalysts for Oxygen Reduction Reaction (ORR). A combination of techniques including UV-Vis-NIR absorption, Raman and X-ray Photoelectron Spectroscopy (XPS) as well as Scanning Electron Microscopy

(SEM) were used to characterize the assembly of the two parts of the functional hybrid system for which the activity and the selectivity toward the ORR process in acidic media are enlightened by a combination of Rotating Disk Electrode (RDE) and Rotating Ring Disk Electrode (RRDE) measurements. The polymerized hybrid (click MWNT-CoCorr) exhibits an overpotential of *ca.* 230 mV compared to a reference platinum ink; the number of electrons involved in the reduction of oxygen is close to 3 in acidic media demonstrating that the corrole cobalt centers in the hybrids reduce oxygen *via* a mix of 2 and 4 electrons pathways.

Introduction

The development of hybrid nanomaterials that preserve and combine the properties of their constituents is a central issue of nanosciences. For more than twenty years, carbon nanomaterials, first carbon nanotubes and then later graphene have drawn attention because of their specific surface area, their aspect ratio (diameter *vs.* length, thickness *vs.* surface), their mechanical properties and among all because of their electronic properties and energy applications.[1-17]

Within the context of renewable energy, the Hydrogen Evolution Reaction (HER), Hydrogen Oxidation Reaction (HOR), Oxygen Evolution Reaction (OER) and Oxygen Reduction Reaction (ORR) are important electrochemical reactions that must be controlled to efficiently fabricate or consume hydrogen and oxygen in fuel cells to produce energy. These reactions require the presence of catalysts like platinum, or platinum group metals (PGM) and the cost and the scarcity of these metals encourage scientists to look for alternatives based on non-noble metal[18-20] or metal-free materials.[13,14,18,21]

In Proton Exchange Membrane Fuel Cells (PEMFCs), the reduction of oxygen is the limiting reaction because of its slow kinetics, the multi-electron process and the competition between the 2-electrons and 4-electrons pathways. In nature, reactions involving the reduction of oxygen are performed by iron porphyrins in the active sites of cytochrome *c* oxidase (CcO). Thus, bioinspired catalysts based on Fe/Cu bimetallic systems, cofacial porphyrins, cofacial corroles or hangman-type systems mimicking the structure of the coenzyme have been synthesized and have been studied for ORR.[22-30] Recently, it appeared that the reduction of oxygen strongly depends on the environment of the catalytic center.[31] Indeed, a bimetallic center (Fe/Cu) is required to perform the reduction of oxygen particularly under rate-limiting electron flux. By

electrochemistry (RDE – rotating disk electrode) in solution or on surface, ‘‘iron-only’’ porphyrins and phthalocyanines are efficient catalysts for the 4-electrons reduction of dioxygen in alkaline or neutral conditions as long as the electron supply is not a limiting factor.[32-35]

Moreover, it was shown that monomeric cobalt MN_4 materials such as Co-phthalocyanines,[33,36,37] Co-porphyrins[33,38] and more recently Co-corroles[39-41] were able to reduce oxygen *via* a mix pathway involving 2 and 4 electrons. In the case of Co-corroles, several works have been dedicated to improve the activity and the selectivity of the catalysts towards the reduction of oxygen. If simple Co-corroles were shown to produce exclusively hydrogen peroxide thanks to a 2-electrons process in solution[42] or after adsorption on edge-plane pyrolytic graphite,[43,44] their ability to catalyse partially and increasingly the 4-electrons process was evidenced after tuning several factors such as the nature of their *meso* and/or *β*-substituents,[45,46] the axial ligation of the pristine cobalt center[47] or by creating very sophisticated corrole based architectures where the active catalyst is linked to a proton relay[30,48,49] or to another cobalt macrocycle.[28,50] One of the crucial step during the 4-electrons ORR is the cleavage of the O-O bond of the peroxo intermediates that requires fast electron transfer from the electrode to the catalytic center.[40] This fast electron transfer is probably the main cause of the enhanced catalytic activity and selectivity resulting from the composite association of Co-corroles and conductive supports such as Fe_3O_4 nanoarrays,[51] high surface area carbon supports[52,53] or carbon nanotubes.[54-56] The immobilization of the catalyst on carbon materials is then ensured using two strategies. The first one rely a simple adsorption of Co-corroles through π-π interactions that was performed by several groups. For example, nanocomposites composed of cobalt(III) tris(pentafluorophenyl)corroles adsorbed on carbon nanotubes were shown to reduce and thereby monitor oxygen in physiological media during in vivo experiments.[57] Because the interactions of

the complexes and the carbon surface are still weak, Lei *et al.* described in 2016 the ORR activity of carbon nanotubes functionalised by a similar complex bearing a peripheral pyrene group introduced to ensure a stronger noncovalent assembly.[55] The second strategy to gather metallocorroles and carbon nanotube is to proceed to a covalent grafting. This grafting requires at first the functionalization of the carbon surface by, for example, ethynyl benzene moieties that were used as linkers to attach co-corroles *via* an azide-alkyne cycloaddtition.[56] If these strategies produced neat composites showing efficient catalytic ORR properties, one cannot exclude that an active layer of adsorbed complexes will be partially lost with time using concentrated acidic environments whereas the robust covalent grafting of molecules transforms hybridized sp^2 carbon atoms into sp^3 ones and induces sizeable decrease of their electronic properties.[58] The aim of the present study is to propose an alternative way of preparing chemically robust Co-corroles-carbon nanotubes conjugates by the creation of a catalyst polymer network around the preserved conducting material and to test the resulting materials for ORR in acid media.

For this purpose, cobalt corroles bearing three propargyl groups on the *meso* positions were designed to be polymerized around Multi Walled Carbon Nanotubes (MWNT) *via* the copper-catalyzed azide-alkyne cycloaddition (CuAAC)[59,60] or Hay coupling.[61] Because the experimental conditions of the latter reaction proved to be too harsh for the active metallocorrole, we focused herein on the formation of core-shell structures *via* CuAAC. The MWNT-CoCorr hybrid materials were characterized by UV-Vis absorption, XPS and Raman spectroscopy and scanning electron microscopy and their electro-catalytic properties were investigated by rotating ring disk electrode (RRDE).

Results and Discussion

The synthesis of the polymerizable cobalt corrole (**CoCorr**) is depicted in Scheme 1 and starts from the 5,10,15-tris(pentafluorophenyl)corrole (**tpfc**) because such *meso* electron-withdrawing groups were shown to induce facilitated Co(III)/Co(II) reductions and improved selectivity toward the 4-electrons reduction of O_2 to give H_2O.[39] Moreover, it was described that the fluorine atoms in *para* position of the *meso*-pentafluorophenyl groups can be easily and selectively substituted by various nucleophilic groups.[62,63] Following the procedure of Wiehe et al.,[62] the triple nucleophilic aromatic substitution of **tpfc** by propargyl alcohol in a basic medium gave the macrocycle **1** bearing three ethynyl moieties in 66% yield (Scheme 1). The subsequent metallation of **1** by $Co(OAc)_2{\cdot}4H_2O$ using classical conditions and in presence of triphenylphosphine (PPh_3) produced the penta-coordinated cobalt complex **CoCorr** in 73% yield.

Scheme 1. Synthetic procedure for Co-corrole (**CoCorr**)[a]

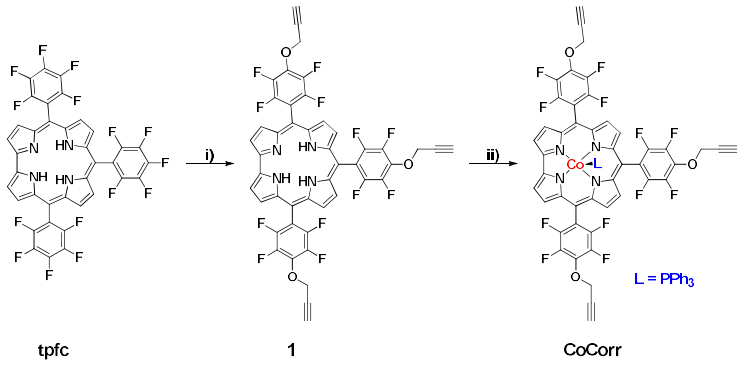

[a](i) Propargyl alcohol, KOH, THF, rt, 18h, 66 %; (ii) $Co(OAc)_2{\cdot}4H_2O$, PPh_3, CH_2Cl_2/MeOH, rt, 10 min, 73%.

The ^1H and ^{19}F NMR spectra of **CoCorr** confirmed the diamagnetism of **CoCorr** (Co^{III}, low-spin d^6) which remains pentacoordinated in solution (see the supporting information). The UV-Vis-NIR spectrum of **CoCorr** recorded in CH_2Cl_2 (Figure S1) is analogous to the one reported

for the complex Co(**tpfc**)PPh_3 and features a split Soret band (346 and 410 nm) and several less intense Q-bands located at 549, 586 and 811 nm. The electrochemical properties of **CoCorr** in CH_2Cl_2 containing 0.1 M of tetra-*n*-butylammonium hexafluorophosphate ($n$$Bu_4NPF_6$) were probed by cyclic voltammetry (Figure S2) and the corresponding redox potential values are given versus the potential of the standard calomel electrode. The cyclic voltammogram of **CoCorr** displays a reversible ligand centered oxidation process at +1.19 V and a reversible reduction at +0.28 V that has been previously attributed to the Co^{III}/Co^{II} couple. The reversibilty of this reduction observed in CH_2Cl_2 is quite unexpected because previous studies using other solvents reported irreversible first reduction processes of phosphine ligated cobalt(II) corroles resulting from the dissociation of the axial phosphine ligand.[64,65]

The synthesis of MWNT-CoCorr hybrid (**click MWNT-CoCorr**) is shown in Scheme 2. Briefly, purified MWNTs[66] were dispersed in *N*,*N*-dimethylformamide (DMF) under argon, then 1,6-diazidohexane,[67] **CoCorr**, $Cu(MeCN)_4PF_6$ and tris(3-hydroxypropyltriazolylmethyl)amine (THPTA)[68] were added. The suspension was stirred at room temperature overnight, filtered through a 0.2 μm PTFE membrane and washed successively with DMF, water, NH_4Cl solution (to remove the copper catalyst), again with water, then ethanol and dichloromethane. As a reference material, we also prepared physisorbed MWNT-CoCorr (**ads MWNT-CoCorr**) by simply mixing MWNT with **CoCorr** in tetrahydrofuran using bath sonication before removal of the solvent using an argon flow.

Scheme 2. Synthetic procedure for the **MWNT-CoCorr hybrids** (**ads MWNT-CoCorr**, **click MWNT-CoCorr**)[a]

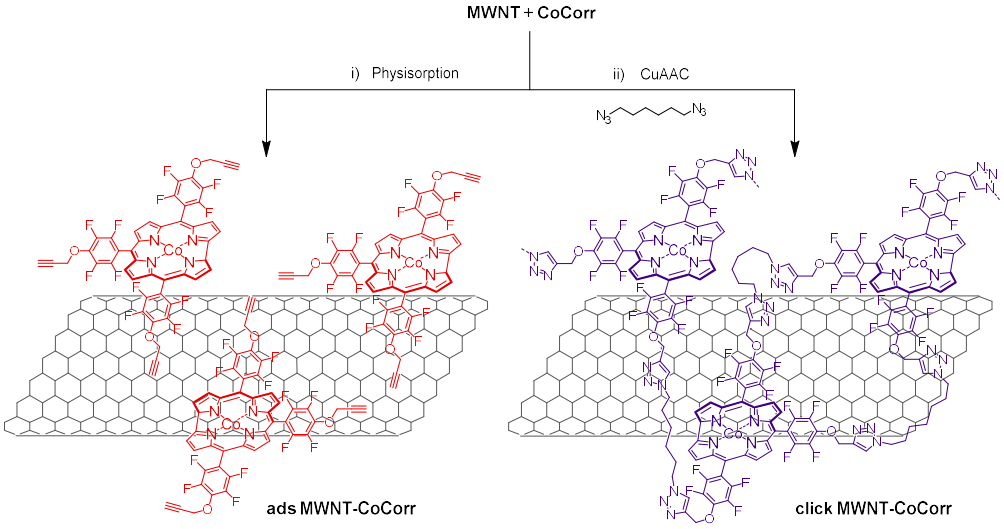

[a](i) THF sonication, rt, 10 min; (ii) 1,6-diazidohexane, $Cu(MeCN)_4PF_6$, THPTA, DMF, rt, overnight.

The **click MWNT-CoCorr** hybrid was characterized by UV-Vis-NIR absorption, Raman and X-ray photoelectron spectroscopies. First the absorption spectra (Figure 1a) show that the spectrum of the **click MWNT-CoCorr** hybrid is the combination of the spectra of **MWNT** and of **CoCorr**. The XPS spectra of the **MWNT** and **click MWNT-CoCorr** hybrid are compared in Figures 1b and 1c. The survey spectra of the **click MWNT-CoCorr** hybrid show (additionally to the presence of carbon and oxygen) the presence of nitrogen, fluorine and cobalt coming from the corrole; the atomic content of cobalt in the hybrid was estimated to 0.15%; this number should be taken with caution since at this low value XPS cannot be quantitative. For comparison, the atomic percentage of cobalt in the **ads MWNT-CoCorr** is 0.69% (calculated from the quantity of **MWNT** and **CoCorr** introduced in the mixture).

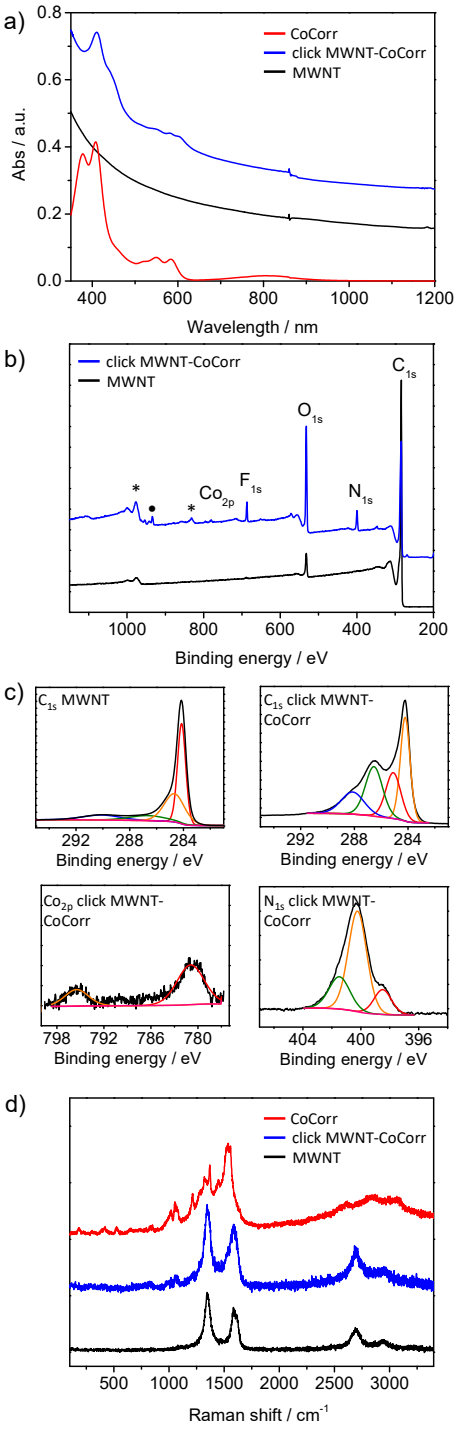

Figure 1. a) Absorption spectra of **CoCorr**, **MWNT** and **click MWNT-CoCorr** hybrid in DMF; b) XPS spectra (survey) of **MWNT** and **click MWNT-CoCorr** hybrid. The peaks labelled * are due to Auger band of oxygen and fluorine and the one with • is due to Co_{2s} and to the presence of

copper from catalyst which was not totally removed probably because of the presence of numerous triazole groups in the hybrids; c) comparison between the C_{1s} high resolution spectra of **MWNT** and **click MWNT-CoCorr** (top), high resolution spectra of Co_{2p} and N_{1s} of **click MWNT-CoCorr**; d) Raman spectra (excitation λ = 532 nm) of **MWNT**, **click MWNT-CoCorr hybrid** and **Co-Corr**.

The Raman spectra recorded with excitation at 532 nm are presented in Figure 1d. The spectrum of **MWNT** shows the typical first order graphitic mode (G band) at 1590 cm^{-1} and the defect band (D band) at 1350 cm^{-1} as well as the second order 2D and D + G in the 2500–3000 cm^{-1} region. The cobalt corrole (in red) exhibits rich features in particular in the 950-1700 cm^{-1} region; some of these bands can be observed on the spectrum of the **click MWNT-CoCorr** hybrid (see the zoom of the spectra of **CoCorr** and **click MWNT-CoCorr** in Figure S3) confirming the presence of corroles on the nanotubes.

The nanotube hybrids were characterized by scanning electron microscopy (SEM). Figure 2 presents the micrographs of two nanotube-corrole hybrids: the **click MWNT-CoCorr** and the **ads MWNT-CoCorr** for which the corrole is simply adsorbed on the nanotube sidewall; the latter hybrid served as reference material for the electrocatalytic studies. The images of the **ads MWNT-CoCorr** clearly show the tubular structures with drop-like aggregates on the nanotubes. This behavior has already been observed for iron porphyrins adsorbed on MWNT;[34] and is due to the segregation between the two components (*i.e.* nanotubes and corroles, in the present case). Therefore, a part of the corrole active species is not properly in contact with the nanotubes. On the contrary, for the **click MWNT-CoCorr** (Figure 2b) no aggregates were detected suggesting that the corroles are homogeneously distributed on the nanotube surfaces.

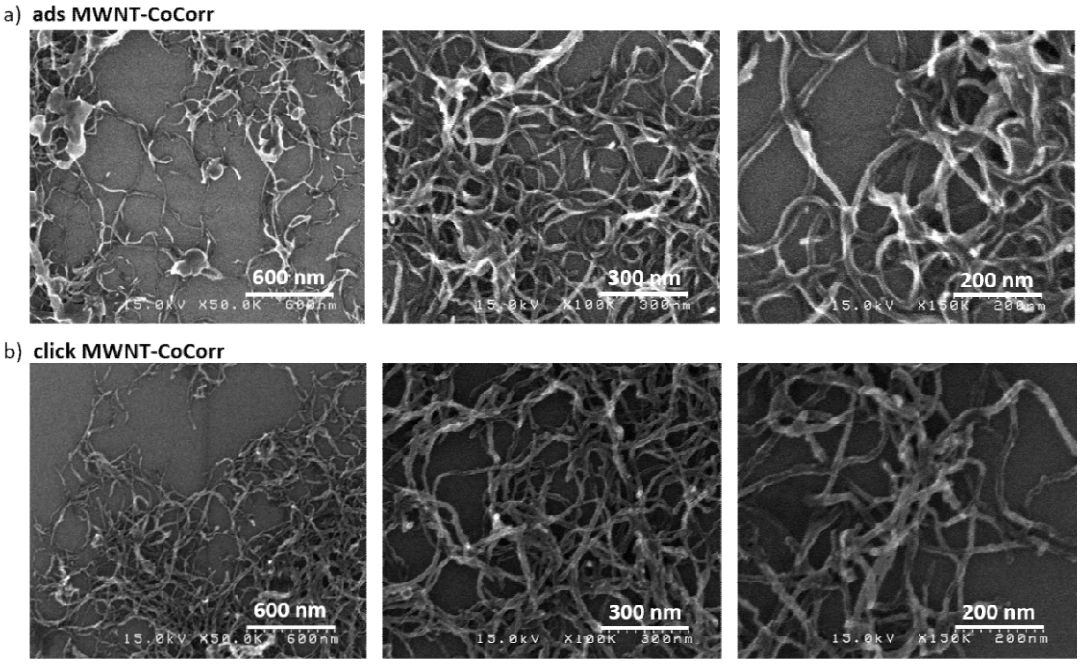

Figure 2. SEM images of a) **ads MWNT-CoCorr** and b) **click MWNT-CoCorr**; in the physisorbed hybrid **ads MWNT-CoCorr**, the corroles tend to segregate and form drop-like aggregates.

We now turn to the electrocatalytic properties of the carbon nanotubes/cobalt corrole hybrids for ORR in acidic medium (0.5 M H_2SO_4). Figures 3a-d present RDE (Rotating Disk Electrode) curves for the reduction of oxygen of the different materials: **CoCorr**, **MWNT**, **ads MWNT-CoCorr** and **click MWNT-CoCorr** mixed with Nafion and deposited on Glassy Carbon (GC) electrodes at pH 0. All the curves correspond to the average (reduction and reoxidation) of the cyclic voltammetry curves.

First, the RDE curves of the simple cobalt corrole (**CoCorr**) show a relatively low activity with an ORR onset potential of *ca.* 40 mV *vs.* Ag/AgCl and a maximum current density of 0.6 $mA \cdot cm^{-2}$ at 2000 rpm (Figure 3a). The nanotubes alone exhibit a similar onset potential but

slightly higher current density of 2 mA·cm^{-2} at 2000 rpm (Figure 3b); it is generally admitted that carbon nanotubes reduce oxygen following a 2-electron process.[69,70] When the corrole is combined to the nanotubes, the ORR activity increases remarkably; indeed **ads MWNT-CoCorr** and **click MWNT-CoCorr** (Figure 3c-d) exhibit onset potentials for ORR of *ca.* 0.40 V and 0.45 V *vs.* Ag/AgCl, respectively. It is worth mentioning that on the same setup and under the same conditions the onset potential for the reduction of oxygen of a reference platinum (Pt/C) ink is 0.70 V *vs.* Ag/AgCl reference electrode (Figure 3e); this means that our best hybrids present an overpotential of 250 mV compared to platinum.

The current density is related to the number of electrons involved in the reduction of oxygen. Thus, the increase of current density for **click MWNT-CoCorr** suggests that the hybrid material ink reduces oxygen *via* a process involving a higher number of electrons than the catalytic inks made only with cobalt corrole. The presence of the nanotubes is therefore extremely important in improving the ORR properties. We believe that this is due to the conductivity of the nanotubes, which facilitates the access of the electrons to the catalytic centers. This result is not surprising, since it was reported, for the case of a series of iron porphyrins deposited on different carbon electrodes, that the mesoscale environment around the catalytic center plays a crucial role in the resulting properties.[31] The limited ORR activity of **ads MWNT-CoCorr** compared to **click MWNT-CoCorr** may be also attributed to the segregation of corrole and the nanotubes in the catalytic ink and therefore to the lack of efficient electron transfer from the nanotube to the corrole to perform the reduction. Figure S4 present the cyclic voltammetry curves of **CoCorr**, **MWNT**, **ads MWNT-CoCorr** and **click MWNT-CoCor**; from these curves it is possible to observe the capacitive current on the materials. We can say that the formation of the covalent network has two effects on the electrochemical response when comparing (**click MWNT-**

CoCorr) to the physisorbed hydrid (**ads MWNT-CoCorr**): the electrochemical surface area seems indeed larger (about 1.5 time according to capacitive current at 0.75V – Figure S4b), but the dominant effect is the decrease of the charge transfer resistance as observable by a shift of 140 mV of the overpotential of the two systems (threshold: −0.5 mA/cm^2). The mechanism is not clear and we believe that it is not the covalent linkage between the corroles that is important but more likely the fact that the corroles are more homogeneously distributed and/or in better contact with the nanotube sidewalls.

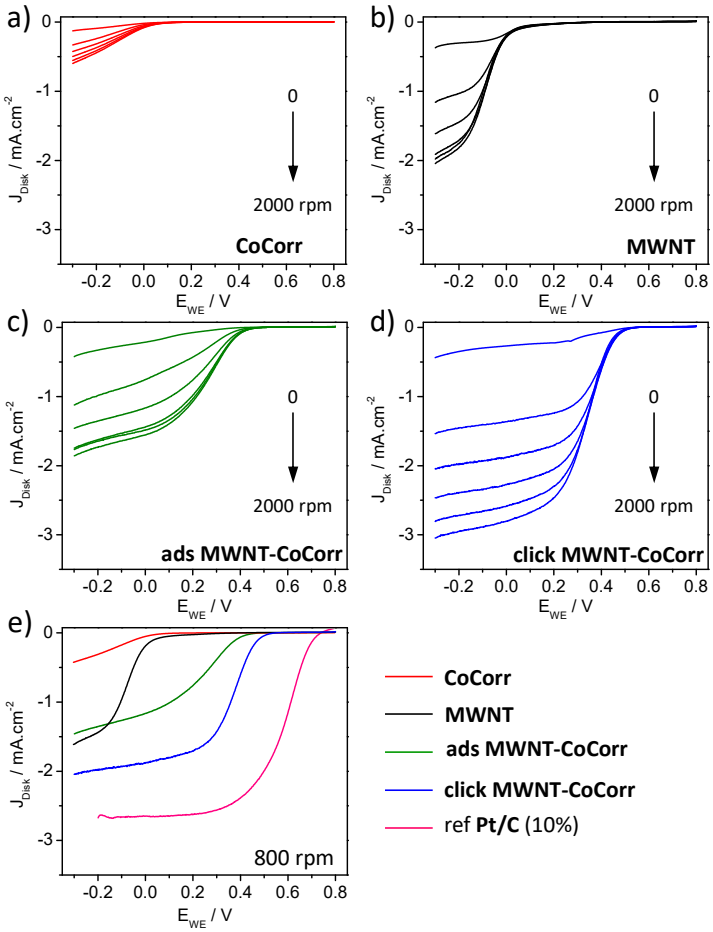

Figure 3. a)-d) RDE curves recorded for ORR in O_2-saturated 0.5 M H_2SO_4 (scan rate = 5 mV·s^{-1}, room temperature) for **CoCorr**, **MWNT**, **ads MWNT-CoCorr** and **click MWNT-**

CoCorr mixed with Nafion and deposited on Glassy Carbon (GC) electrodes for rotation speeds of 0, 400, 800, 1200, 1600 and 2000 rpm; the potential are given vs. Ag/AgCl; e) comparison between the RDE curves at 800 rpm of **CoCorr**, **MWNT**, **ads MWNT-CoCorr**, **click MWNT-CoCorr** and a reference platinum ink.

The number of electrons involved in the reduction of oxygen was determined for the **click MWNT-CoCorr** hybrid by RRDE and using Koutecky-Levich equation (Eq. 1) with Levich analysis (Eq 2).[71]

$$\frac{1}{J} = \frac{1}{J_k} + \frac{1}{J_{MT}} \quad \text{[Eq. 1]}$$

$$J_{MT} = -0.620nFC_{O_2}D_{O2}^{\frac{2}{3}}\upsilon^{-\frac{1}{6}}\omega^{\frac{1}{2}} \quad \text{[Eq. 2]}$$

With J the measured current, J_k the kinetic current, J_{MT} the mass transport current in [Eq. 1] and n the number of electron involved in the reduction of oxygen, F the Faraday's constant (96 485.34 $C \cdot mol^{-1}$), C_{O2} the concentration of oxygen ($1.1 \cdot 10^{-6}$ $mol \cdot cm^{-3}$), D_{O2} the diffusion coefficient of oxygen in aqueous solution ($1.4 \cdot 10^{-5}$ $cm^2 \cdot s^{-1}$), ν the kinematic viscosity (0.01 $cm^2 \cdot s^{-1}$)[72] and ω the rotation speed ($rad \cdot s^{-1}$). The K-L plot determined at different potentials (0.0, −0.1, −0.2 and −0.3 V *vs* Ag/AgCl) on the RDE curves of **click MWNT-CoCorr** (see Figure 3d) is shown in Figure 4a. Using the Levich analysis [Eq. 2], we determined that the number of electrons involved in the reduction of oxygen was of 3.20 at −0.3 V and it dropped regularly to 2.7 electrons at 0.0 V (Figure 4b); the values are summarized in Table 1.

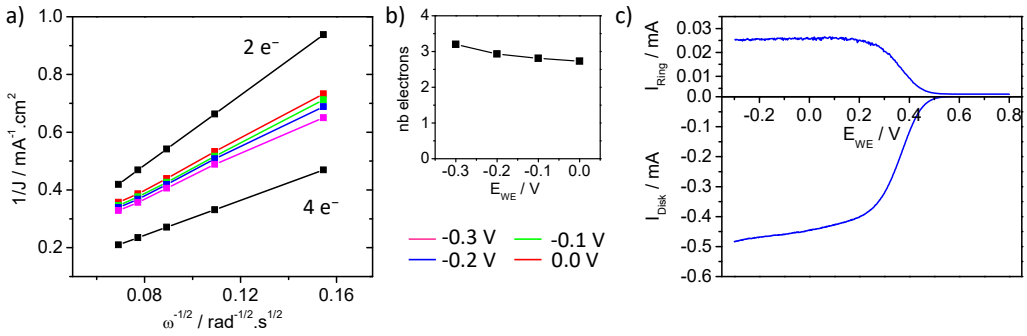

Figure 4. a) K-L plots at different potential −0.3 V (pink), −0.2 V (blue), −0.1 V (green) and 0.0 V (red) vs. Ag/AgCl determined from the RDE curves for **click MWNT-CoCorr**; b) number of electrons determined using the Levich analysis as a function of the disk potential (Working Electrode); c) RRDE curves for the reduction of oxygen (negative current) and for the oxidation of hydrogen peroxide (positive current) at a rotation rate of 1200 rpm for **click MWNT-CoCorr** in O_2-saturated 0.5M H_2SO_4. The ring electrode was polarized at 1.2 V vs. Ag/AgCl; scan rate: 5 mV s^{-1}.

The number of electrons involved in the reaction can also be determined by monitoring the oxidation of the hydrogen peroxide produced by the catalyst at the disk by the ring electrodes. The RRDE measurement at a rotation rate of 1200 rpm is given in Figure 4c. The number of electrons involved in the reduction of oxygen can be deduced from [Eq. 3]:

$$n = \frac{4I_{disk}}{I_{disk}+\frac{I_{ring}}{N_C}} \qquad \text{[Eq. 3]}$$

N_C, the collection coefficient (0.2) was determined using the one-electron $Fe(CN)_6^{3-}/Fe(CN)_6^{4-}$ redox couple and I_{disk} and I_{ring} were determined on the RRDE curves. We determined the variation of the number of electrons from the curves at 1200 rpm (Figure 4c) at different potentials (from −0.3 to +0.1V *vs.* Ag/AgCl); the corresponding value goes from 3.17 to 3.07. The number of electrons involved in the reduction are collected in Table 1.

The RRDE curves for **CoCorr** and **ads MWNT-CoCorr** are given in Figure S5. For the catalytic inks made of these materials, the number of electrons involved in the reduction of oxygen is 3.25 and 3.36, respectively. These values are determined at −0.3V *vs.* Ag/AgCl for a rotation rate of 1200 rpm, they are very similar to the one of **click MWNT-CoCorr**.

Table 1. Number of electrons involved in the reduction of oxygen by the **click MWNT-CoCorr** hybrids determined using the K-L plots and by RRDE at −0.3V vs. Ag/AgCl.

	K-L plots (at different E_{WE} / V)				RRDE 1200 rpm (at different E_{WE} / V)				
click MWNT-CoCorr	−0.3	−0.2	−0.1	0.0	−0.3	−0.2	−0.1	0.0	0.1
Nb electrons	3.20	2.94	2.81	2.73	3.17	3.14	3.12	3.11	3.07

By RRDE and Koutecky-Levich analyses, we estimated that the number of electrons involved in the reduction of oxygen is around three. The cobalt corroles reduce oxygen *via* a mix of two and four electrons process and therefore produce hydrogen peroxide. The formation of "face-to-face"-like multilayers of cobalt corrole around the nanotubes could improve the reduction process as we have shown for a multilayer of cobalt porphyrins around carbon nanotubes.[66]

Conclusion

Here, we described the ORR activity of MWNT-CoCorr hybrids prepared by the unprecedented polymerization of poly-alkynyl cobalt corroles around carbon nanotubes through multiple CuAAC. This polymerization ensures i) a chemical stability of the composite catalysts by excluding the partial loss of the active layer by desorption and ii) an improved cohesion

between the two partners by preventing the segregation between the two components when their assembly results only from π-π interactions.

While iron tetraphenylporphyrin or iron phthalocyanine are extremely simple and efficient catalysts for 4-electron oxygen reduction in alkaline media; their ORR activity rapidly degrades in 0.5M H_2SO_4. Therefore, the development of materials compatible with acidic media, which is the environment in PEMFC, is strongly needed. The ORR activity of the **click MWNT-CoCorr** hybrid combines the properties of each component. This activity rely on a mix pathway involving 2 and 4 electrons and therefore has a selectivity towards the 4-electrons ORR process that remains modest with an overpotential of 230 mV (for **click MWNT-CoCorr**) compared to i) the reference platinum ink and to ii) previous hybrids systems gathering carbon supports and analogous cobalt corroles for which the number of electrons involved in the reduction of oxygen could reach 3.6 in acidic media.[55,56] Previous and recent results have shown that the compactness of adsorbed Co-corroles[49,53] or the length of the linking arm[73] when they are grafted are crucial to get improved ORR selectivity when they are associated to carbon support. In the present work, the moderate selectivity probably results from the bulkyness of the complexes and the flexibility of their polymers that increase the average distance between the active sites and the nanotubes. However, these materials are paving the way for preparing analogous and robust hybrid ORR catalysts by using polymerization as an alternative way of gathering the conducting and active layers.

Supporting Information

Synthesis of the corroles derivatives and the carbon nanotube hybrids, characterization and additional figures; these materials are available free of charge.

Corresponding Authors

Stéphane Campidelli

stephane.campidelli@cea.fr

Gabriel Canard

gabriel.canard@univ-amu.fr

Author Contributions

The manuscript was written through contributions of all authors. All authors have given approval to the final version of the manuscript.

Acknowledgement

This work was supported by the JST-ANR program TMOL "Molecular Technology" project MECANO (ANR-14-JTIC-0002-01) and by a public grant overseen by the French National Research Agency (ANR) as part of the "Investissements d'Avenir" program (Labex NanoSaclay, reference: ANR-10-LABX-0035).

References

(1) Hirsch, A. The era of carbon allotropes. *Nat. Mater.* **2010**, *9*, 868-871.

(2) Avouris, P.; Chen, Z.; Perebeinos, V. Carbon-based electronics. *Nat. Nanotechnol.* **2007**, *2*, 605-615.

(3) Islam, A. E.; Rogers, J. A.; Alam, M. A. Recent Progress in Obtaining Semiconducting Single-Walled Carbon Nanotubes for Transistor Applications. *Adv. Mater.* **2015**, *27*, 7908-7937.

(4) Peng, L.-M.; Zhang, Z.; Qiu, C. Carbon nanotube digital electronics. *Nat. Electron.* **2019**, *2*, 499-505.

(5) Castro Neto, A. H.; Guinea, F.; Peres, N. M. R.; Novoselov, K. S.; Geim, A. K. The electronic properties of graphene. *Rev. Mod. Phys.* **2009**, *81*, 109-162.

(6) Schwierz, F. Graphene transistors. *Nat. Nanotechnol.* **2010**, *5*, 487-496.

(7) Punetha, V. D.; Rana, S.; Yoo, H. J.; Chaurasia, A.; McLeskey Jr, J. T.; Ramasamy, M. S.; Sahoo, N. G.; Cho, J. W. Functionalization of carbon nanomaterials for advanced polymer nanocomposites: A comparison study between CNT and graphene. *Prog. Polym. Sci* **2017**, *67*, 1-47.

(8) Ellis, J. E.; Star, A. Carbon Nanotube Based Gas Sensors toward Breath Analysis. *ChemPlusChem* **2016**, *81*, 1248-1265.

(9) Brennan, L. J.; Byrne, M. T.; Bari, M.; Gun'ko, Y. Carbon Nanomaterials for Dye-Sensitized Solar Cell Applications: A Bright Future. *Adv. Energy Mater.* **2011**, *1*, 472-485.

(10) Zhang, A.; Lieber, C. M. Nano-Bioelectronics. *Chem. Rev.* **2016**, *116*, 215-257.

(11) Jariwala, D.; Sangwan, V. K.; Lauhon, L. J.; Marks, T. J.; Hersam, M. C. Carbon nanomaterials for electronics, optoelectronics, photovoltaics, and sensing. *Chem. Soc. Rev.* **2013**, *42*, 2824-2860.

(12) Wen, L.; Li, F.; Cheng, H.-M. Carbon Nanotubes and Graphene for Flexible Electrochemical Energy Storage: from Materials to Devices. *Adv. Mater.* **2016**, *28*, 4306-4337.

(13) Inagaki, M.; Toyoda, M.; Soneda, Y.; Morishita, T. Nitrogen-doped carbon materials. *Carbon* **2018**, *132*, 104-140.

(14) Xu, Y.; Kraft, M.; Xu, R. Metal-free carbonaceous electrocatalysts and photocatalysts for water splitting. *Chem. Soc. Rev.* **2016**, *45*, 3039-3052.

(15) Xu, C.; Xu, B.; Gu, Y.; Xiong, Z.; Sun, J.; Zhao, X. S. Graphene-based electrodes for electrochemical energy storage. *Energy Environ. Sci.* **2013**, *6*, 1388-1414.

(16) Li, J.-C.; Hou, P.-X.; Liu, C. Heteroatom-Doped Carbon Nanotube and Graphene-Based Electrocatalysts for Oxygen Reduction Reaction. *Small* **2017**, *13*, 1702002.

(17) Fang, R.; Chen, K.; Yin, L.; Sun, Z.; Li, F.; Cheng, H.-M. The Regulating Role of Carbon Nanotubes and Graphene in Lithium-Ion and Lithium–Sulfur Batteries. *Adv. Mater.* **2019**, *31*, 1800863.

(18) Morozan, A.; Jousselme, B.; Palacin, S. Low-platinum and platinum-free catalysts for the oxygen reduction reaction at fuel cell cathodes. *Energy Environ. Sci.* **2011**, *4*, 1238-1254.

(19) Xia, W.; Mahmood, A.; Liang, Z.; Zou, R.; Guo, S. Earth-Abundant Nanomaterials for Oxygen Reduction. *Angew. Chem. Int. Ed.* **2016**, *55*, 2650-2676.

(20) Zhang, W.; Lai, W.; Cao, R. Energy-Related Small Molecule Activation Reactions: Oxygen Reduction and Hydrogen and Oxygen Evolution Reactions Catalyzed by Porphyrin- and Corrole-Based Systems. *Chem. Rev.* **2017**, *117*, 3717-3797.

(21) Hu, C.; Dai, L. Carbon-Based Metal-Free Catalysts for Electrocatalysis beyond the ORR. *Angew. Chem. Int. Ed.* **2016**, *55*, 11736-11758.

(22) Collman, J. P.; Fu, L.; Herrmann, P. C.; Zhang, X. A Functional Model Related to Cytochrome c Oxidase and Its Electrocatalytic Four-Electron Reduction of O_2. *Science* **1997**, *275*, 949-951.

(23) Collman, J. P.; Devaraj, N. K.; Decréau, R. A.; Yang, Y.; Yan, Y.-L.; Ebina, W.; Eberspacher, T. A.; Chidsey, C. E. D. Cytochrome c Oxidase Model Catalyzes Oxygen to Water Reduction Under Rate-Limiting Electron Flux. *Science* **2007**, *315*, 1565-1568.

(24) Collman, J. P.; Denisevich, P.; Konai, Y.; Marrocco, M.; Koval, C.; Anson, F. C. Electrode Catalysis of the Four-Electron Reduction of Oxygen to Water by Dicobalt Face-to-Face Porphyrins. *J. Am. Chem. Soc.* **1980**, *102*, 6027-6036.

(25) Ricard, D.; Andrioletti, B.; L'Her, M.; Boitrel, B. Electrocatalytic reduction of dioxygen to water by tren-capped porphyrins, functional models of cytochrome *c* oxidase. *Chem. Commun.* **1999**, 1523-1524.

(26) Chang, C. K.; Liu, H. Y.; Abdalmuhdi, I. Electroreduction of Oxygen by Pillared Cobalt Cofacial Diporphyrin Catalysts. *J. Am. Chem. Soc.* **1984**, *106*, 2725-2726.

(27) Chang, C. J.; Loh, Z.-H.; Shi, C.; Anson, F. C.; Nocera, D. G. Targeted Proton Delivery in the Catalyzed Reduction of Oxygen to Water by Bimetallic Pacman Porphyrins. *J. Am. Chem. Soc.* **2004**, *126*, 10013-10020.

(28) Kadish, K. M.; Frémond, L.; Ou, Z.; Shao, J.; Shi, C.; Anson, F. C.; Burdet, F.; Gros, C. P.; Barbe, J.-M.; Guilard, R. Cobalt(III) Corroles as Electrocatalysts for the Reduction of Dioxygen: Reactivity of a Monocorrole, Biscorroles, and Porphyrin-Corrole Dyads. *J. Am. Chem. Soc.* **2005**, *127*, 5625-5631.

(29) McGuire Jr, R.; Dogutan, D. K.; Teets, T. S.; Suntivich, J.; Shao-Horn, Y.; Nocera, D. G. Oxygen reduction reactivity of cobalt (II) hangman porphyrins. *Chem. Sci.* **2010**, *1*, 411-414.

(30) Dogutan, D. K.; Stoian, S. A.; McGuire Jr, R.; Schwalbe, M.; Teets, T. S.; Nocera, D. G. Hangman Corroles: Efficient Synthesis and Oxygen Reaction Chemistry. *J. Am. Chem. Soc.* **2011**, *133*, 131-140.

(31) Rigsby, M. L.; Wasylenko, D. J.; Pegis, M. L.; Mayer, J. M. Medium Effects Are as Important as Catalyst Design for Selectivity in Electrocatalytic Oxygen Reduction by Iron Porphyrin Complexes. *J. Am. Chem. Soc.* **2015**, *137*, 4296-4299.

(32) Ricard, D.; L'Her, M.; Richard, P.; Boitrel, B. Iron porphyrins as models of cytochrome *c* oxidase. *Chem. Eur. J.* **2001**, *7*, 3291-3297.

(33) Morozan, A.; Campidelli, S.; Filoramo, A.; Jousselme, B.; Palacin, S. Catalytic activity of cobalt and iron phthalocyanines or porphyrins supported on different carbon nanotubes towards oxygen reduction reaction. *Carbon* **2011**, *49*, 4839-4847.

(34) Hanana, M.; Arcostanzo, H.; Das, P. K.; Bouget, M.; Le Gac, S.; Okuno, H.; Cornut, R.; Jousselme, B.; Dorcet, V.; Boitrel, B.; Campidelli, S. Synergic effect on oxygen reduction reaction of strapped iron porphyrins polymerized around carbon nanotubes. *New J. Chem.* **2018**, *42*, 19749-19754.

(35) Boitrel, B.; Bouget, M.; Das, P. K.; Le Gac, S.; Roisnel, T.; Hanana, M.; Arcostanzo, H.; Cornut, R.; Jousselme, B.; Campidelli, S. Oxygen reduction reaction catalyzed by overhanging carboxylic acid strapped iron porphyrins adsorbed on carbon nanotubes. *J. Porphyr. Phthalocyanines* **2020**, *24*, 675-684.

(36) Jasinski, R. A New Fuel Cell Cathode Catalyst. *Nature* **1964**, *201*, 1212-1213.

(37) Zagal, J.; Páez, M.; Tanaka, A. A.; Dos Santos, J. R.; Likous, C. A. Electrocatalytic activity of metal phthalocyanines for oxygen reduction. *J. Electroanal. Chem.* **1992**, *339*, 13-30.

(38) Collman, J. P.; Marrocco, M.; Denisevich, P.; Koval, C.; Anson, F. C. Potent catalysis of the electroreduction of oxygen to water by dicobal porphyrin dimers on graphite electrodes. *J. Electroanal. Chem.* **1979**, *101*, 117-122.

(39) Lei, H.; Li, X.; Meng, J.; Zheng, H.; Zhang, W.; Cao, R. Structure Effects of Metal Corroles on Energy-Related Small Molecule Activation Reactions. *ACS Catal.* **2019**, *9*, 4320-4344.

(40) Li, Y.; Wang, N.; Lei, H.; Li, X.; Zheng, H.; Wang, H.; Zhang, W.; Cao, R. Bioinspired N_4-metallomacrocycles for electrocatalytic oxygen reduction reaction. *Coord. Chem. Rev.* **2021**, *442*, 213996.

(41) Lei, H.; Zhang, Q.; Liang, Z.; Guo, H.; Wang, Y.; Lv, H.; Li, X.; Zhang, W.; Apfel, U.-P.; Cao, R. Metal-Corrole-Based Porous Organic Polymers for Electrocatalytic Oxygen Reduction and Evolution Reactions. *Angew. Chem. Int. Ed.* **2022**, *61*, e202201104.

(42) Rana, A.; Lee, Y.-M.; Li, X.; Cao, R.; Fukuzumi, S.; Nam, W. Highly Efficient Catalytic Two-Electron Two-Proton Reduction of Dioxygen to Hydrogen Peroxide with a Cobalt Corrole Complex. *ACS Catal.* **2021**, *11*, 3073-3083.

(43) Kadish, K. M.; Shen, J.; Frémond, L.; Chen, P.; El Ojaimi, M.; Chkounda, M.; Gros, C. P.; Barbe, J.-M.; Ohkubo, K.; Fukuzumi, S.; Guilard, R. Clarification of the Oxidation State of Cobalt Corroles in Heterogeneous and Homogeneous Catalytic Reduction of Dioxygen. *Inorg. Chem.* **2008**, *47*, 6726-6737.

(44) Tang, J.; Ou, Z.; Ye, L.; Yuan, M.; Fang, Y.; Xue, Z.; Kadish, K. M. Meso-dichlorophenyl substituted Co(III) corrole: A selective electrocatalyst for the two-electron reduction of dioxygen in acid media, X-ray crystal structure analysis and electrochemistry. *J. Porphyr. Phthalocyanines* **2014**, *18*, 891-898.

(45) Schechter, A.; Stanevsky, M.; Mahammed, A.; Gross, Z. Four-Electron Oxygen Reduction by Brominated Cobalt Corrole. *Inorg. Chem.* **2012**, *51*, 22-24.

(46) Ou, Z.; Ou, Z.; Meng, D.; Tang, J.; Fang, Y.; Liu, R.; Kadish, K. M. Cobalt triarylcorroles containing one, two or three nitro groups. Effect of NO_2 substitution on electrochemical properties and catalytic activity for reduction of molecular oxygen in acid media. *J. Inorg. Biochem.* **2014**, *136*, 130-139.

(47) Meng, J.; Lei, H.; Li, X.; Zhang, W.; Cao, R. The Trans Axial Ligand Effect on Oxygen Reduction. Immobilization Method May Weaken Catalyst Design for Electrocatalytic Performance. *J. Phys. Chem. C* **2020**, *124*, 16324-16331.

(48) Han, J.; Wang, N.; Li, X.; Cao, R. Improving Electrocatalytic Oxygen Reduction Activity and Selectivity with a Cobalt Corrole Appended with Multiple Positively Charged Proton Relay Sites. *J. Phys. Chem. C* **2021**, *125*, 24805-24813.

(49) Friedman, A.; Reddy Samala, N.; Honig, H. C.; Tasior, M.; Gryko, D. T.; Elbaz, L.; Grinberg, I. Control of Molecular Catalysts for Oxygen Reduction by Variation of pH and Functional Groups. *ChemSusChem* **2021**, *14*, 1886-1892.

(50) Kadish, K. M.; Frémond, L.; Shen, J.; Chen, P.; Ohkubo, K.; Fukuzumi, S.; El Ojaimi, M.; Gros, C. P.; Barbe, J.-M.; Guilard, R. Catalytic Activity of Biscobalt Porphyrin-Corrole Dyads Toward the Reduction of Dioxygen. *Inorg. Chem.* **2009**, *48*, 2571-2582.

(51) Xie, L.; Li, X.; Wang, B.; Meng, J.; Lei, H.; Zhang, W.; Cao, R. Molecular Engineering of a 3D Self-Supported Electrode for Oxygen Electrocatalysis in Neutral Media. *Angew. Chem. Int. Ed.* **2019**, *58*, 18883-18887.

(52) Levy, N.; Shpilman, J. S.; Honig, H. C.; Major, D. T.; Elbaz, L. A surprising substituent effect in corroles on the electrochemical activation of oxygen reduction. *Chem. Commun.* **2017**, *53*, 12942-12945.

(53) Honig, H. C.; Friedman, A.; Zion, N.; Elbaz, L. Enhancement of the oxygen reduction reaction electrocatalytic activity of metallo-corroles using contracted cobalt(iii) CF_3-corrole incorporated in a high surface area carbon support. *Chem. Commun.* **2020**, *56*, 8627-8630.

(54) Wang, Z.; Lei, H.; Cao, R.; Zhang, M. Cobalt Corrole on Carbon Nanotube as a Synergistic Catalyst for Oxygen Reduction Reaction in Acid Media. *Electrochem. Acta* **2015**, *171*, 81-88.

(55) Lei, H.; Liu, C.; Wang, Z.; Zhang, Z.; Zhang, M.; Chang, X.; Zhang, W.; Cao, R. Noncovalent Immobilization of a Pyrene-Modified Cobalt Corrole on Carbon Supports for Enhanced Electrocatalytic Oxygen Reduction and Oxygen Evolution in Aqueous Solutions. *ACS Catal.* **2016**, *6*, 6429-6437.

(56) Meng, J.; Lei, H.; Li, X.; Qi, J.; Zhang, W.; Cao, R. Attaching Cobalt Corroles onto Carbon Nanotubes: Verification of Four-Electron Oxygen Reduction by Mononuclear Cobalt Complexes with Significantly Improved Efficiency. *ACS Catal.* **2019**, *9*, 4551-4560.

(57) Liu, X.; Feng, T.; Ji, W.; Wang, Z.; Zhang, M. A cobalt corrole/carbon nanotube enables simultaneous electrochemical monitoring of oxygen and ascorbic acid in the rat brain. *Analyst* **2020**, *145*, 70-75.

(58) Cognet, L.; Tsyboulski, D. A.; Rocha, J.-D. R.; Doyle, C. D.; Tour, J. M.; Weisman, R. B. Stepwise Quenching of Exciton Fluorescence in Carbon Nanotubes by Single-Molecule Reactions. *Science* **2007**, *316*, 1465-1468.

(59) Rostovtsev, V. V.; Green, L. G.; Fokin, V. V.; Sharpless, K. B. A Stepwise Huisgen Cycloaddition Process: Copper(I)-Catalyzed Regioselective "Ligation" of Azides and Terminal Alkynes. *Angew. Chem. Int. Ed.* **2002**, *41*, 2596-2599.

(60) Tornøe, C. W.; Christensen, C.; Meldal, M. Peptidotriazoles on Solid Phase: [1,2,3]-Triazoles by Regiospecific Copper(I)-Catalyzed 1,3-Dipolar Cycloadditions of Terminal Alkynes to Azides. *J. Org. Chem.* **2002**, *67*, 3057-3064.

(61) Chalifoux, W. A.; Tykwinski, R. R. Synthesis of extended polyynes: Toward carbyne. *C. R. Chimie* **2009**, *12*, 341-358.

(62) Golf, H. R. A.; Reissig, H.-R.; Wiehe, A. Regioselective Nucleophilic Aromatic Substitution Reaction of meso -Pentafluorophenyl-Substituted Porphyrinoids with Alcohols. *Eur. J. Org. Chem.* **2015**, 1548-1568.

(63) Gross, Z.; Galili, N.; Saltsman, I. The First Direct Synthesis of Corroles fromPyrrole. *Angew. Chem. Int. Ed.* **1999**, *38*, 1427-1429.

(64) Adamian, V. A.; D'Souza, F.; Licoccia, S.; Di Vona, M. L.; Tassoni, E.; Paolesse, R.; Boschi, T.; Kadish, K. M. Synthesis, Characterization, and Electrochemical Behavior of (5,10,15-Tri-X-phenyl-2,3,7,8,12,13,17,18-octamethylcorrolato)cobalt(III) Triphenylphosphine Complexes, Where X = p-OCH_3, p-CH_3, p-Cl, m-Cl, o-Cl, m-F, or o-F. *Inorg. Chem.* **1995**, *34*, 532-540.

(65) Mahammed, A.; Giladi, I.; Goldberg, I.; Gross, Z. Synthesis and Structural Characterization of a Novel Covalently-Bound Corrole Dimer. *Chem. Eur. J.* **2001**, *7*, 4259-4265.

(66) Hijazi, I.; Bourgeteau, T.; Cornut, R.; Morozan, A.; Filoramo, A.; Leroy, J.; Derycke, V.; Jousselme, B.; Campidelli, S. Carbon Nanotube-Templated Synthesis of Covalent Porphyrin Network for Oxygen Reduction Reaction. *J. Am. Chem. Soc.* **2014**, *136*, 6348-6354.

(67) Díaz, D. D.; Rajagopal, K.; Strable, E.; Schneider, J.; Finn, M. G. "Click" Chemistry in a Supramolecular Environment: Stabilization of Organogels by Copper(I)-Catalyzed Azide-Alkyne [3 + 2] Cycloaddition. *J. Am. Chem. Soc.* **2006**, *128*, 6056-6057.

(68) Liu, X.-M.; Thakur, A.; Wang, D. Efficient Synthesis of Linear Multifunctional Poly(ethylene glycol) by Copper(I)-Catalyzed Huisgen 1,3-Dipolar Cycloaddition. *Biomacromolecules* **2007**, *8*, 2653-2658.

(69) Alexeyeva, N.; Tammeveski, K. Electrochemical Reduction of Oxygen on Multiwalled Carbon Nanotube Modified Glassy Carbon Electrodes in Acid Media. *Electrochem. Solid-State Lett.* **2007**, *10*, F18-F21.

(70) Kruusenberg, I.; Alexeyeva, N.; Tammeveski, K. The pH-dependence of oxygen reduction on multi-walled carbon nanotube modified glassy carbon electrodes. *Carbon* **2009**, *47*, 651-658.

(71) Zhou, R.; Zheng, Y.; Jaroniec, M.; Qiao, S.-Z. Determination of the Electron Transfer Number for the Oxygen Reduction Reaction: From Theory to Experiment. *ACS Catal.* **2016**, *6*, 4720-4728.

(72) Lu, G.; Yang, H.; Zhu, Y.; Huggins, T.; Ren, Z. J.; Liu, Z.; Zhang, W. Synthesis of a conjugated porous Co(II) porphyrinylene-ethynylene framework through alkyne metathesis and its catalytic activity study. *J. Mater. Chem. A* **2015**, *3*, 4954-4959.

(73) Li, X.; Lei, H.; Liu, J.; Zhao, X.; Ding, S.; Zhang, Z.; Tao, X.; Zhang, W.; Wang, W.; Zheng, X.; Cao, R. Carbon Nanotubes with Cobalt Corroles For Hydrogen and Oxygen Evolution in pH 0-14 Solutions. *Angew. Chem. Int. Ed.* **2018**, *57*, 15070-15075.

Table of contents